

A Quantum Approximate Optimization Algorithm Based on CNR Operations

Da You Lv and An Min Wang^{a)}

*Department of Modern Physics, University of Science and Technology of China,
China*

This paper introduces the “comparison and replacement” (CNR) operation and constructs a pure quantum approximate algorithm for combinatorial optimization problems which depends on the number of level p and ancilla qubits number of CNR t . CNR lifts the probability of strings with high object function level by level in the algorithm, which ensures the strings approximately maximizing the object function dominate the probability. When the number of bits n remains unchanged, the performance of the algorithm improves with the increase of p directly. And t determines the accuracy and reliability of CNR. The practical performance of algorithm trends to theoretical results as t increases. For fixed p and t , the algorithm outputs a state with identical probability distribution of measurement or the corresponding fit curve for nondegenerate or degenerate instance respectively, which means that, for universal combinatorial optimization problems, the algorithm always works.

^{a)}Corresponding author; Electronic mail: anmwang@ustc.edu.cn

I. INTRODUCTION

Quantum computation can accelerate approximate optimization and promotes the birth of relative algorithms, which solve the exponential inefficiency of combinatorial optimization problem fundamentally. The performance of quantum optimization shows the quantum supremacy¹⁻³ compared with classical algorithm. The beginning is that Edward Farhi et. al develops the quantum adiabatic algorithm (QAA)⁴ and introduces the quantum approximate optimization algorithm (QAOA)⁵ relies on the parameters produced by classical procedure. He and his partners investigate applications of p -level QAOA in different combinatorial optimization problems such as typical instances⁶⁻⁹, Sherrington-Kirkpatrick model¹⁰ and ensemble of k -edge graphs¹¹. The results present outstanding properties such as concentration^{10,11}. And QAOA shows great application prospect in transportation science¹², economy¹³, product synthesis in biochemistry¹⁴ and specific physics system¹⁵⁻¹⁷ etc. And we introduce a pure quantum algorithm for approximate optimization in this paper.

For a combinatorial optimization problem, the object function depends on m clauses, which can be written in the form of

$$C(z) = \sum_{a=1}^m C_a(z), \quad (1)$$

where C_a is the a -th clause. And the discrete variable encoded as a n -bit string $z = z_1 z_2 \cdots z_n \in \{0, 1\}^n$. The object function is assigned to a Hermitian operator \mathcal{C} as the function of Z , the z -axis spin operator of $\frac{1}{2}$ particle. The eigenvalue equation is

$$\mathcal{C} |z\rangle = C(z) |z\rangle, \quad (2)$$

where computational bases $\{|z\rangle\}$ encode the strings z in the way that the j -th bit z_j is encoded with the j -th qubit which is an eigenstate $|z_j\rangle \in \{|0\rangle, |1\rangle\}$ of Z according to eigenvalue directly. The main body of algorithm is a unitary operation that transforms an efficiently prepared initial state into a $|z^*\rangle$ with approximation ratio defined as

$$r = \frac{\langle \mathcal{C} \rangle - C_{min}}{C_{max} - C_{min}}, \quad (3)$$

where $\langle \mathcal{C} \rangle$ is the expectation of \mathcal{C} to $|z^*\rangle$, close to 1 as possible in polynomial steps. The last step is to measure $|z^*\rangle$ and obtain a string approximately maximizing the object function with high probability.

In this paper, our algorithm presents a typical divide-and-conquer structure determined by the number of level p of CNR operations with t ancilla qubits. We give recursion relations only influenced by the degeneracy of object function to calculate the probability distribution of measurement and theoretical performance and the reference lower bound for t . Then we summarize the practical performance in random instances of degenerate and nondegenerate problems, which shows

$$r_p \leq r_{p-1} \quad (4)$$

$$\lim_{p \rightarrow \infty} r_p = 1. \quad (5)$$

The equal sign of (4) is taken in trivial cases. For fixed n and p , the theoretical probability distribution of final measurement is nearly identical except the degeneracy influence, which means the amplification for probability of obtaining a string well optimizing is independent of problem.

The paper is organized as follows. In section II, We introduce p -level algorithm constructed with CNR and implement it in detail. And we derive the recursion relations for probability distribution about p and give a bound for p -level algorithm in section III. Then we study the application in MAX-2-XOR and 2-edge graphs with Gaussian weights and investigate the average performance dependence on p and t separately in section IV. We conclude the performance and property of the algorithm in section V.

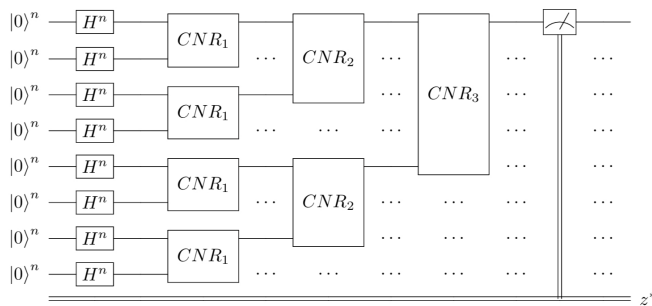


Figure 1: The divide-and-conquer structure of the 3-level algorithm. We omit the ancilla qubits of CNR and each quantum wire delivers n -qubit state for simplification.

II. ALGORITHM BASED ON COMPARISON AND REPLACEMENT

The sketch of our algorithm is shown in Figure 1. Restricted by the quantum no-cloning theory, the p -level algorithm presents a typical divide-and-conquer structure

with 2^p register in $|0\rangle^n$ state initially and corresponding number of ancilla qubits initially transformed into uniform superposition by Hadamard gates to keep inputs in each level identical.

As the sketch shows, in the k -th level, 2^{p-k+1} identical target registers from the $(k-1)$ -th level enter as inputs and they are divided into new target and support register pairs. Then 2^{p-k} CNR operations transforms them and delivers 2^{p-k} target registers to the $(k+1)$ -th level. For p -level algorithm, there are 2^p CNR operations in the algorithm finishing in p steps. We will show the performance dependence on p in theory and practice in section III 1 and IV 2, which is also the important motivation for us to construct the algorithm in the form above.

1. Comparison with t ancilla qubits

Quantum comparison is designed as a operation that can compare two computational bases and store the answer in an available qubit or register. With technique in quantum phase estimation^{18,19}, quantum comparer can be realized. Our initial state is the tensor product of two arbitrary n -qubit state, $|T\rangle$ and $|S\rangle$ named target and support register separately, and ancilla register with t ancilla qubits in uniform superposition state. First we assume that $|T\rangle$ and $|S\rangle$ store two n -qubit computational bases $|z_s\rangle$ and $|z_t\rangle$ separately. Consider the operation $\mathcal{D} = \mathcal{C} \otimes I - I \otimes \mathcal{C}$ and generate the unitary operation

$$\exp\left(i\frac{\mathcal{D}}{M}\right) = \exp\left(i\frac{\mathcal{C}_t}{M}\right) \otimes \exp\left(-i\frac{\mathcal{C}_s}{M}\right), \quad (6)$$

where \mathcal{C}_t and \mathcal{C}_s only act on the $|T\rangle$ and $|S\rangle$. It is necessary to scale spectrum of \mathcal{D} in the range $[-\pi, \pi)$ to avoid periodicity of exponent on the imaginary axis. We introduce a scale factor M that satisfies

$$M \geq \frac{C_{max} - C_{min}}{2\pi} \quad (7)$$

It is a strict bound of M for the performance of comparison. A suitable M can be easily estimated from function value range for graphs with weights in specific distribution, such as Gaussian-weight graph and MAX-k-XOR. The procedure of comparison in detail is as follows. We impose a phase on $|T\rangle |S\rangle$ with the help of ancilla qubits and act the inverse Quantum Fourier transformation on $2n+t$ qubits, which redistributes the probability of measuring the computational bases in t ancilla qubits. The brief procedure in explicit

form is

$$|T\rangle |S\rangle \sum_{x=-2^{t-1}}^{2^{t-1}-1} |x\rangle \rightarrow \sum_{x=-2^{t-1}}^{2^{t-1}-1} e^{i2\pi \frac{C(z_s) - C(z_t)}{M} x} |T\rangle |S\rangle |x\rangle \rightarrow |T\rangle |S\rangle |\tilde{a}\rangle \quad (8)$$

where ancilla computational bases $\{|x\rangle\}$ are encoded in the same of the computational bases of initial Hilbert space. In this paper, we use the decimal value to label computational bases of ancilla qubits for simplification. The whole procedure leaves $|V_a\rangle$ unchanged and stores information in ancilla qubits $|\tilde{a}\rangle$. The final probability distribution of each computational basis in $|\tilde{a}\rangle$ is

$$Pr(y) = \frac{1}{2^{2t}} \frac{1 - \cos(2\pi(2^t a - y))}{1 - \cos(2\pi(a - \frac{y}{2^t}))} \quad (9)$$

corresponding to decimal value y , which peaks at $\frac{2^t a}{2\pi}$ as Figure 2.

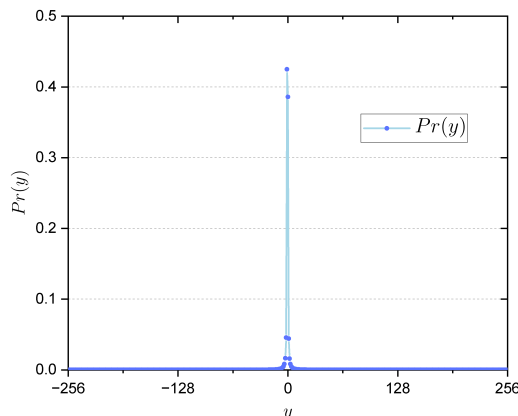


Figure 2: The final probability distribution of measuring $|\tilde{a}\rangle$, when $a = 0.001$ and $t = 9$.

In practical application, it is useful to preset an accuracy b to simplify the optimization. Accuracy is the quantity that preset a tolerable error between the result and true value. The difference less than accuracy can be seen negligible. For MAX-k-XOR or MAX-k-SAT, gaps of object function value are greater than 2, therefore we can choose $b = \frac{1}{2|E|}$ simply. As to graphs where weights obeys continuous distribution, it is necessary to consider the acceptable error of the practical condition. We will discuss the further relation between accuracy and ancilla qubits number t in III 2.

For single computational basis in each register, comparison outputs $(2n + 1)$ -qubit state in which $|z_t\rangle$ and $|z_s\rangle$ are unchanged and the first ancilla qubit indicates the string

with greater object function value stored in target and support register. If the ancilla qubit is in $|0\rangle$, comparison guesses the computational basis in $|T\rangle$, z_t is the string with a greater object function value, and if it is in $|1\rangle$, comparison guesses the string z_s in $|S\rangle$ has a greater object function value. Each step shown above is unitary, so it still works when $|T\rangle$ and $|S\rangle$ store the superposition of computational bases and the first ancilla qubit delivers the information of tensor product of computational bases in the same way according to distribute law separately.

It is worth noting that comparison is probabilistic procedure. For fixed eigenvalue a , the distribution (9) is only determined by t . In principle, we can calculate the probability of comparison outputting correct answer. In section III 2, we discuss the relation among t , accuracy and probability of success and give the lower bound of t for p -level algorithm.

2. Replacement

Replacement is designed to adjust the tensor product according to the information from comparison. It is straightforward to utilize the available ancilla qubit via controlled operation. We introduce the overwriting operation and the quantum circuit is shown in Figure 3. Overwriting covers $|\alpha\rangle$ with $|\beta\rangle$ only at the cost of the certainty of the original $|\beta\rangle$. And we implement the replacement by controlled n -qubit overwriting which are

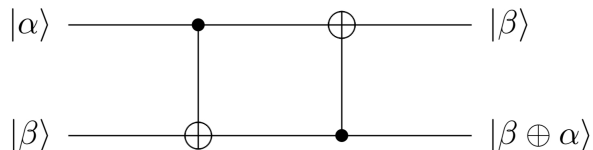


Figure 3: The quantum circuit of 1-qubit overwriting operation.

n simultaneous 1-qubit overwritings controlled by the ancilla qubit. For the case that $|T\rangle$ and $|S\rangle$ only store the computational bases $|z_t\rangle$ and $|z_s\rangle$, replacement ensures that finally $|T\rangle$ stores the computational basis according to greater object function value in $|z_t\rangle$ and $|z_s\rangle$. Because the replacement is unitary, it still works for general $|T\rangle$ and $|S\rangle$.

III. THEORETICAL PERFORMANCE OF ALGORITHM

The algorithm depends on p directly because of the divide-and-conquer structure, and the performance of comparison is determined with ancilla qubits number t . We analyze the performance of CNR in general cases assuming that every CNR succeeds. And we give a lower bound of t with which the assumption can be fulfilled by repeating statistically. The results of this section are heuristic and important for the application of our algorithm. It is mechanics of our algorithm to approximately optimize any none trivial instances.

1. The recursion relation of probability

The object operation \mathcal{C} can be understood as a Hamiltonian. Relabel the computational basis according to energy in descending order, the state in target and support registers can be rewritten in the following form

$$|T\rangle = \sum_{i=1}^G \sum_{j=1}^{g_i} k_{i;j} |E_{i;j}\rangle, \quad (10)$$

$$|T\rangle = \sum_{p=1}^G \sum_{q=1}^{g_p} l_{p;q} |E_{p;q}\rangle. \quad (11)$$

It assume that there are G energy levels and the i -th energy level has g_i eigenstates. In principal, writing initial states in the form of (10) and (11) requires complete knowledge about object function, however it is not necessary to CNR. The probability of computational bases in the a -th energy level is

$$\begin{aligned} Pr(a, 1) &= \sum_{j=1}^{g_a} \sum_{p \geq a} \sum_{q=1}^{g_p} |k_{a;j} l_{p;q}|^2 + \sum_{i \geq a} \sum_{j=1}^{g_i} \sum_{q=1}^{g_a} |k_{i;j} l_{a;q}|^2 \\ &= \sum_{j=1}^{g_a} |k_{a;j}|^2 + \sum_{q=1}^{g_a} |l_{a;q}|^2 - \sum_{i \leq a} \sum_{j=1}^{g_i} \sum_{q=1}^{g_a} |k_{i;j} l_{a;q}|^2 \\ &\quad - \sum_{j=1}^{g_a} \sum_{p \leq a} \sum_{q=1}^{g_p} |k_{a;j} l_{p;q}|^2 + \sum_{j=1}^{g_a} \sum_{q=1}^{g_a} |k_{a;j} l_{a;q}|^2, \end{aligned} \quad (12)$$

The sums in (12) are meaningful. We define the probability of a -th energy level after k CNR as $Pr(a, k)$ and the sum from $Pr(1, k)$ to $Pr(a, k)$ as $S(a, k)$ for $|z_t\rangle$, and $Pr'(a, k)$

and $S'(a, k)$ for $|z_s\rangle$ similarly. Then we have

$$\begin{aligned} Pr(a, 1) &= Pr(a, 0) + Pr'(a, 0) + Pr(a, 0)Pr'(a, 0) \\ &\quad - Pr(a, 0)S'(a, 0) - Pr'(a, k)S(a, k) \end{aligned} \quad (13)$$

When $|T\rangle$ is always identical to $|S\rangle$, the same as our algorithm, equation (13) constitutes the recurrent relation

$$Pr(a, k) = 2Pr(a, k-1) + Pr(a, k-1)^2 - 2Pr(a, k-1)S(a, k-1), \quad (14)$$

$$S(a, k) = 1 - (1 - S(a, k-1))^2 = 1 - (1 - S(a, 0))^{2k}, \quad (15)$$

where we remove the prime. We can calculate the probability of every energy level after p -level algorithm using (14) and (15). The n -bit strings with greater object function value dominate the probability distribution finally by the limit

$$\lim_{n \rightarrow \infty} \left(1 - \frac{1}{n}\right)^n = \frac{1}{e} \quad (16)$$

and the monotonicity of $(1 - \frac{1}{n})^n$. In our algorithm, $S(2^{n-p}, p)$ increases to $1 - \frac{1}{e} \approx 0.6321$ at least. Recursion relations (14) and (15) provide the theoretical basis for our algorithm. The derivation above is independent of the numerical value of each energy level. Thus the recursion relation is reliable for universal object function.

2. The lower bound of ancilla qubits number

Assuming the difference of object function between two strings is a , comparison fails when the measurement l have different sign with a . The amplitude of $|l\rangle$ in final ancilla state is

$$\alpha_l = \frac{1}{2^t} \frac{1 - \exp(i2\pi(2^t a - l))}{1 - \exp(i2\pi(a - \frac{l}{2^t}))}. \quad (17)$$

And l is an integer in the range $[-2^{t-1}, 2^{t-1})$. For any real θ ,

$$|1 - \exp(i\theta)| \leq 2. \quad (18)$$

Whenever $-\pi \leq \theta \leq \pi$,

$$|1 - \exp(i\theta)| \geq 2|\theta|. \quad (19)$$

To meet a worst case, we consider that $b = a = -2^s$. The probability satisfies the inequality

$$|\alpha_l|^2 \leq \frac{1}{4(2^{t-s} - l)^2}. \quad (20)$$

And we obtain a sequence of equations and inequalities

$$\begin{aligned} Pr(l \geq 0) &\leq \sum_{l=0}^{2^{t-1}-1} \frac{1}{4(2^{t-s}-l)^2} = \frac{1}{4(2^{t-s})^2} + \sum_{l=1}^{2^{t-1}-1} \frac{1}{4(2^{t-s}-l)^2} \\ &\leq \frac{1}{4(2^{t-s})^2} + \int_0^{+\infty} \frac{1}{4(2^{t-s}-l)^2} dl = \frac{1}{4(2^{t-s})^2} + \frac{1}{4(2^{t-s})} \leq \frac{1}{2(2^{t-s})}. \end{aligned} \quad (21)$$

Introduce a tolerable bound ϵ for probability of the situation that comparison fails, the important inequality is

$$\frac{1}{2(2^{t-s})} \leq \epsilon. \quad (22)$$

And the solution is

$$t = s + \left\lceil \log\left(\frac{1}{2\epsilon}\right) \right\rceil, \quad (23)$$

which is the lower bound of t , and $1 - \epsilon$ is the preset lower bound probability of success.

For fixed p , the algorithm consists of $2^p - 1$ CNR operations. If every comparison succeeds, the recursion relations can be used to our algorithm directly. Considering (16), if probability of success is $1 - \frac{1}{2^p-1}$, the probability of every comparison succeeding will increase to $\frac{1}{e} \approx 0.3679$. Thus the lower bound is

$$t = s + p - 1. \quad (24)$$

And with the numerical calculation, if we prepare one more ancilla qubit, the probability of complete success is at least $\sqrt{\frac{1}{e}} \approx 0.6059$. To sum up, we give a reference lower bound of t for p -level algorithm that

$$t = s + p. \quad (25)$$

We only need to repeat the whole algorithm $O(1)$ times statistically for any n to meet the theoretical performance. The influence of t on p -level algorithm will be shown in section IV 3 with figures.

IV. APPLICATION AND PRACTICAL PERFORMANCE

In this section, we study the application in MAX-2-XOR and 2-edge graphs with Gaussian weights, and investigate the performance dependence on p and t .

1. Application in degenerate and nondegenerate cases

Each term in the object function of MAX-k-XOR is XOR. The corresponding Hermitian operator omitting constant is

$$\mathcal{C} = \sum_{\{q_1 \dots q_k\} \subset \{1, 2, \dots, n\}} d_{q_1 \dots q_k} Z_{q_1} \dots Z_{q_k}, \quad (26)$$

where each $d_{q_1 \dots q_k} \in \{0, -1\}$. The object function is extremely degenerate. Figure 4 shows the value structure of a 10-bit MAX-2-XOR random instance and the corresponding probability distribution of output after 1, 2 and 3-level algorithm, where the density of -1 in coefficients (edge density) is 0.6 and t is large enough. Here we label each string in descending order of object function value. It can be seen that CNR re-

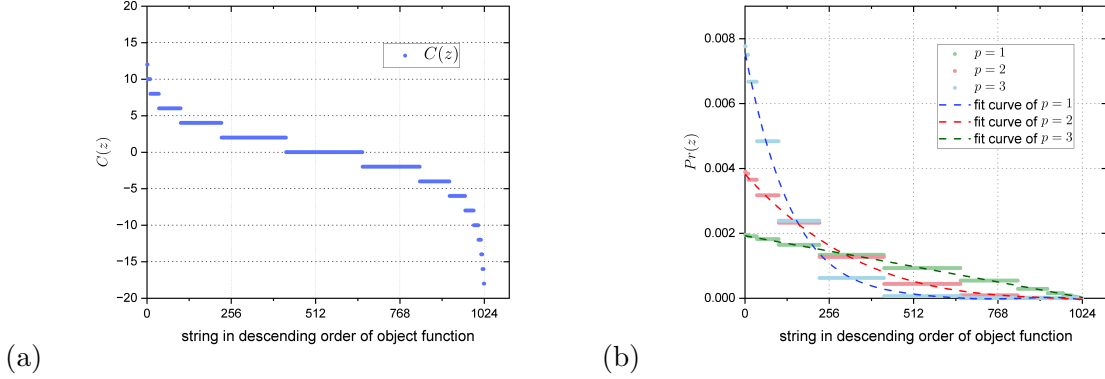


Figure 4: (a) The scatter graph of object function value to a MAX-2-XOR random instance, where $n = 10$ and edge density is 0.6. (b) The scatter graph of probability of measuring labeled string in descending order when applied the algorithm with $p=1, 2$ and 3 for the instance and corresponding fit curves.

flect the degeneracy in probability. In the scatter plots for p from 1 to 3, the algorithm concentrate more probability on the strings with greater object function value.

The Hermitian object operator of Gaussian-weight 2-edge graph is

$$\mathcal{C} = \sum_{i, j \in \{1, 2, \dots, n\}} d_{ij} Z_i Z_j, \quad (27)$$

where $d_{ij} \sim N(0, 1)$. The degeneracy occurs in much lower probability in this case. In Figure 5, we plot object function value structure and scatter graph and fit curves

of probability distribution for $p = 1, 2, 3$ in a random Gaussian-weight 2-edge graph instance. And we also choose a large t . Figure 4 and 5 shows the different degeneracy obviously. From the fit curves in Figure 4(b) and Figure 5(b), fit curves of probability changing with the increase of p is identical. And the behavior for these two instances satisfies the recursion relations (14) and (15) strictly.

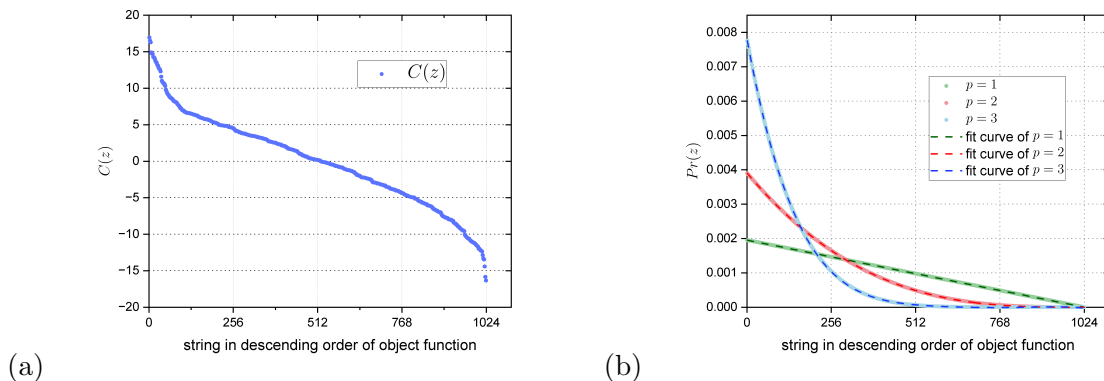


Figure 5: (a) The scatter graph of object function value to a Gaussian-weight 2-edge instance when $n = 10$. (b) The scatter graph of probability of measuring labeled string when applied the algorithm with $p=1, 2$ and 3 for the instance and corresponding fit curves.

To sum up, if t is large enough, the algorithm makes the strings with greater object function value dominate the probability, whether the problem is degenerate or not. And the fit curves is perfectly matched with the recursion relations, which confirms the conclusions in section III 1.

2. Performance depend on the number of level p

With the discussion in section III, the redistribution is identical, but according to (3) the performance is a functional of object function. Thus we estimate the average performance of the algorithm for reliability at this occasion. Initial approximation ratio $r_{initial}$ of random instance floats in a range, which means the analysis of final approximation ratio r is not reliable. We introduce the approximation rate defined as

$$X_r = \frac{r - r_{initial}}{1 - r_{initial}}. \quad (28)$$

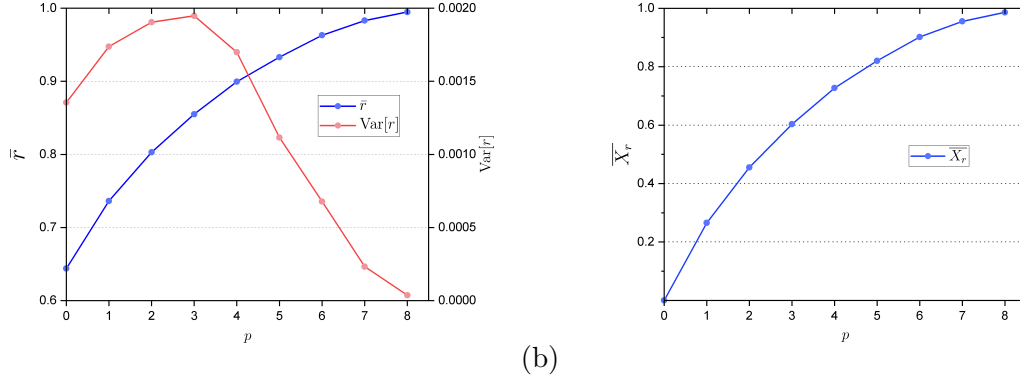


Figure 6: (a) Our result that the average approximation ratio and its variance about MAX-2-XOR with $n = 8$ and edge density is 0.5. And t is large enough. (b) The average approximation rate curve with p increasing.

To quantify the average performance, we focus on average approximation ratio \bar{r} , variance of approximation ratio $\text{Var}[r]$ and average approximation rate \bar{X}_r . We generate 1000 random instances of MAX-2-XOR with $n = 8$, and t is large enough to make the error only from instances and edge density is 0.5. Our result is shown in Figure 6.

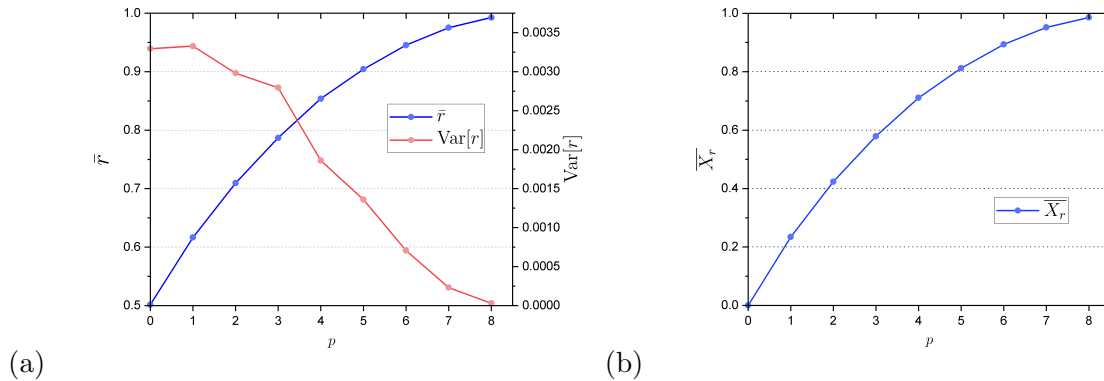


Figure 7: (a) When $n = 8$, the average approximation ratio and variance of Gaussian-weight 2-edge graph instances as t is large enough. (b) The average approximation rate curve along with p increasing.

As p increases to n , \bar{r} and \bar{X}_r increase steadily to near 1 and $\text{Var}[r]$ floats at first then decreases rapidly to 0. When p is low, the \bar{r} increase and keeps \bar{X}_r about 0.26 for each level of CNR. We also plot the result for 2-edge graphs with Gaussian weights, for

$n = 8$ and big enough t , on 1000 random instances.

From IV 1, MAX-2-XOR and 2-edge graphs with Gaussian weights are two problems with extremely different degeneracy. As we have shown, $r_{initial}$ of the two problems have significant difference. We should pay more attention to X_r . $\overline{X_r}$ of each step is also near 0.26 when p is low. When p increase to a considerable value, difference of performance is reduced to a negligible degree. And the performance at low p is also considerable.

3. Performance depends on number of ancilla qubits t

We give a lower bound for the number of ancilla qubits t in (23). Consider the 3-level algorithm applied to an 8-qubit Gaussian-weight 2-edge instance, we investigate

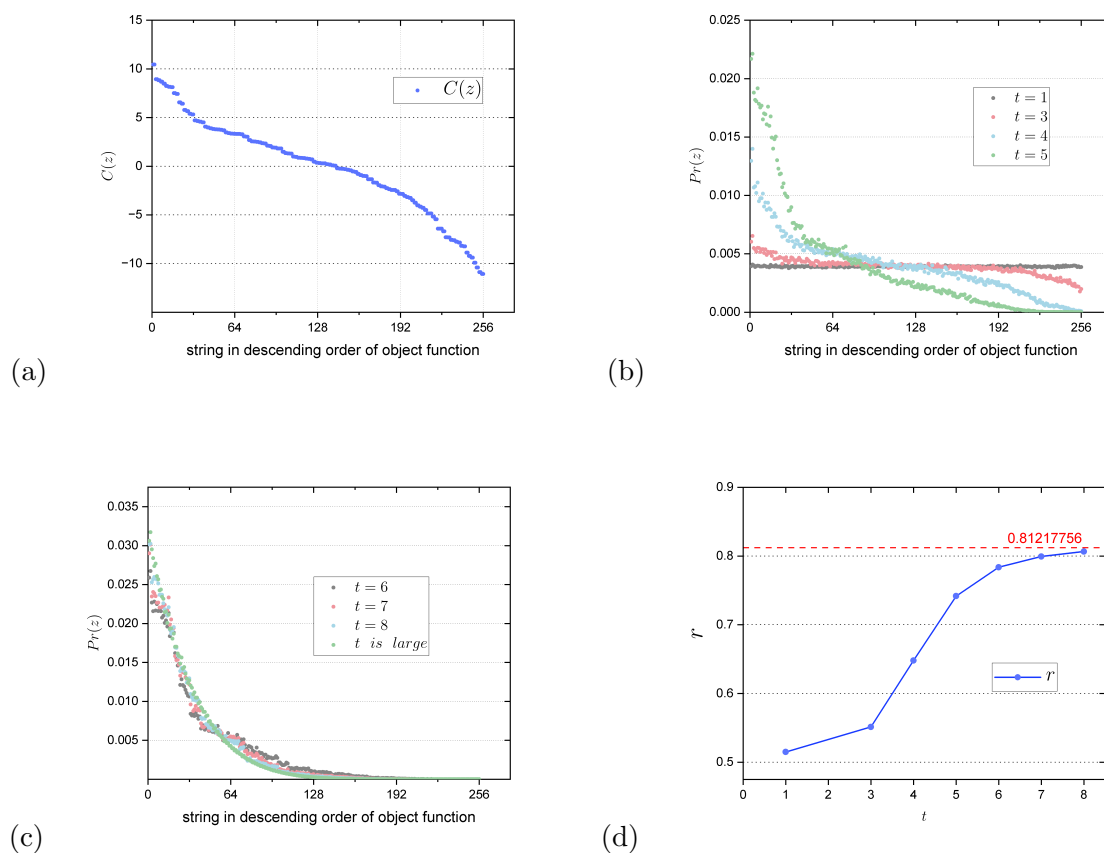


Figure 8: (a) The value structure of object function. (b) The probability distribution of strings when $t = 1, 3, 4, 5$. (c) The probability distribution of strings when $t = 6, 7, 8$ and t is large. (d) The approximation ratio changing along with t from 1 to 8 and the theoretical approximation ratio.

the lower bound of t in this instance. Figure 8 consists of the value structure (a), the scatter graph of probability distribution for $t = 1, 3, 4$ and 5 and $t = 6, 7, 8$ and theoretical case in (b)(c), and plots r in (d). It can be seen that, as t increases, the probability distribution changes from uniform superposition to the theoretical curve. And from (d) the approximation ratio increases and reaches a slow-growth stage at $t = 6$ and at this point is 0.7837, which is very close to the theoretical approximation ratio 0.8122. From the result in (23) and discussions in section IV, the theoretical lower bound of t is $s + 3$, which can be seen from that comparing (b) and (c), probability distribution when $t \leq 4$ has obvious different shape of scatter graph. And $\text{Var}[r]$ on specific instance can be negligible. To sum up, t has a direct influence on the practical approximation ratio, as (d) shows.

V. CONCLUSION

We introduce a pure quantum approximate algorithm based on CNR operation in this paper for universal combinatorial optimization problem in divide-and-conquer structure. We design CNR to compare the object function value of different n -bit strings, and always cover $|T\rangle$ with the n -bit string with greater object function value. The algorithm depends on 2 parameters, p and t . The theoretical probability distribution after p -level algorithm satisfies the recurrent relations

$$Pr(a, k) = 2Pr(a, k - 1) + Pr(a, k)^2 - 2Pr(a, k - 1)S(a, k - 1) \quad (29)$$

$$S(a, k) = 1 - (1 - S(a, k - 1))^2 = 1 - (1 - S(a, 0))^{2k}. \quad (30)$$

And for any p , we can choose a suitable number of ancilla qubits to maintain a reasonable probability of success to ensure number of repetition is $O(1)$ statistically, which is

$$t = s + p, \quad (31)$$

where s is the logarithm accuracy. Moreover, the recursion relation is independent of problem, therefore the algorithm can be used to approximately optimize arbitrary combinatorial optimization problems and obtain a string with great object function with high probability.

When applied to MAX-2-XOR and 2-edge graphs with Gaussian weights, the algorithm shows considerable r and $\overline{X_r}$ rate even when p is small. Though performance is influenced by the problems, \bar{r} and $\overline{X_r}$ trend to 1 and variance decays rapidly as p grows.

The choice of p and t is independent. The qubit number required initially for our p -level algorithm is $O(n2^p + t2^p)$. The whole algorithm needs $O(p)$ CNR steps. And each CNR consists of $O(t^2)$ gates. The freedom of choosing p and t provides initiative for users. However, considering the performance and efficiency, it would be best that users have a basic understanding to specific problem.

ACKNOWLEDGMENTS

This work was supported by National Key R& D Program of China under Grant No. 2018YFB1601402-2.

REFERENCES

- ¹E. Farhi and A. W. Harrow, “Quantum supremacy through the quantum approximate optimization algorithm,” (2019), [arXiv:1602.07674 \[quant-ph\]](#).
- ²S. Hadfield, Z. Wang, B. O’Gorman, E. Rieffel, D. Venturelli, and R. Biswas, “From the quantum approximate optimization algorithm to a quantum alternating operator ansatz,” [Algorithms](#) **12**, 34 (2019).
- ³R. Herrman, P. C. Lotshaw, J. Ostrowski, T. S. Humble, and G. Siopsis, “Multi-angle quantum approximate optimization algorithm,” (2021), [arXiv:2109.11455 \[quant-ph\]](#).
- ⁴E. Farhi, J. Goldstone, S. Gutmann, and M. Sipser, “Quantum computation by adiabatic evolution,” (2000), [arXiv:quant-ph/0001106 \[quant-ph\]](#).
- ⁵E. Farhi, J. Goldstone, and S. Gutmann, “A quantum approximate optimization algorithm,” (2014), [arXiv:1411.4028 \[quant-ph\]](#).
- ⁶Z. Wang, S. Hadfield, Z. Jiang, and E. G. Rieffel, “Quantum approximate optimization algorithm for MaxCut: A fermionic view,” [Physical Review A](#) **97** (2018), [10.1103/physreva.97.022304](#).
- ⁷E. Farhi, J. Goldstone, and S. Gutmann, “A quantum approximate optimization algorithm applied to a bounded occurrence constraint problem,” (2015), [arXiv:1412.6062 \[quant-ph\]](#).

- ⁸C. Y.-Y. Lin and Y. Zhu, “Performance of qaoa on typical instances of constraint satisfaction problems with bounded degree,” (2016), [arXiv:1601.01744 \[quant-ph\]](#).
- ⁹F. G. S. L. Brandao, M. Broughton, E. Farhi, S. Gutmann, and H. Neven, “For fixed control parameters the quantum approximate optimization algorithm’s objective function value concentrates for typical instances,” (2018), [arXiv:1812.04170 \[quant-ph\]](#).
- ¹⁰E. Farhi, J. Goldstone, S. Gutmann, and L. Zhou, “The quantum approximate optimization algorithm and the sherrington-kirkpatrick model at infinite size,” [Quantum](#) **6**, 759 (2022).
- ¹¹J. Basso, D. Gamarnik, S. Mei, and L. Zhou, “Performance and limitations of the QAOA at constant levels on large sparse hypergraphs and spin glass models,” in [2022 IEEE 63rd Annual Symposium on Foundations of Computer Science \(FOCS\)](#) (IEEE, 2022).
- ¹²U. Azad, B. K. Behera, E. A. Ahmed, P. K. Panigrahi, and A. Farouk, “Solving vehicle routing problem using quantum approximate optimization algorithm,” [IEEE Transactions on Intelligent Transportation Systems](#) **24**, 7564–7573 (2023).
- ¹³D. Amaro, M. Rosenkranz, N. Fitzpatrick, K. Hirano, and M. Fiorentini, “A case study of variational quantum algorithms for a job shop scheduling problem,” [EPJ Quantum Technology](#) **9** (2022), [10.1140/epjqt/s40507-022-00123-4](#).
- ¹⁴S. Boulebnane, X. Lucas, A. Meyder, S. Adaszewski, and A. Montanaro, “Peptide conformational sampling using the quantum approximate optimization algorithm,” (2022), [arXiv:2204.01821 \[quant-ph\]](#).
- ¹⁵A. Ozaeta, W. van Dam, and P. L. McMahon, “Expectation values from the single-layer quantum approximate optimization algorithm on ising problems,” [Quantum Science and Technology](#) **7**, 045036 (2022).
- ¹⁶A. E. Alaoui, A. Montanari, and M. Sellke, “Optimization of mean-field spin glasses,” (2020), [arXiv:2001.00904 \[math.PR\]](#).
- ¹⁷P. Chandarana, N. N. Hegade, K. Paul, F. Albarrá n-Arriagada, E. Solano, A. del Campo, and X. Chen, “Digitized-counterdiabatic quantum approximate optimization algorithm,” [Physical Review Research](#) **4** (2022), [10.1103/physrevresearch.4.013141](#).
- ¹⁸R. Cleve, A. Ekert, C. Macchiavello, and M. Mosca, “Quantum algorithms revisited,” [Proceedings of the Royal Society of London. Series A: Mathematical, Physical and](#)

[Engineering Sciences](#) **454**, 339–354 (1998).

- ¹⁹M. Faizan and M. Faryad, “Simulation and analysis of quantum phase estimation algorithm in the presence of incoherent quantum noise channels,” (2023), [arXiv:2307.15675 \[quant-ph\]](#).